Solid State Communications 202 (2015) 19–23

Contents lists available at ScienceDirect

Solid State Communications

journal homepage: www.elsevier.com/locate/ssc

Ab initio study of electronic density of state and photoabsorption of $Ga_{1-x}Mn_xAs$ under pressure

Prayoonsak Pluengphon [a,*], Thiti Bovornratanaraks [b,c], Sornthep Vannarat [d], Udomsilp Pinsook [b,c]

[a] Division of Physical Science, Faculty of Science and Technology, Huachiew Chalermprakiet University, Samutprakarn 10540, Thailand
[b] Extreme Conditions Physics Research Laboratory, Department of Physics, Faculty of Science, Chulalongkorn University, Bangkok 10330, Thailand
[c] ThEP Center, CHE, 328 Si-Ayuttaya Road, Bangkok 10400, Thailand
[d] Large-Scale Simulation Research Laboratory, National Electronics and Computer Technology Center, Pathumthani 12120, Thailand

ARTICLE INFO

Article history:
Received 1 July 2014
Received in revised form
8 October 2014
Accepted 14 October 2014
Communicated by "L. Brey"
Available online 11 November 2014

ABSTRACT

Ab initio calculation based on density functional theory was performed for studying high-pressure effects on the electronic properties and photoabsorption of $Ga_{1-x}Mn_xAs$. Mn atom was substituted into the varied GaAs super cells, which observed the Mn concentrations at 3.70%, 8.33% and 12.50%. In zinc blende phase of $Ga_{1-x}Mn_xAs$, we found that the effects of Mn on GaAs in the pressure range 0–10 GPa are the reducing of band gap, generating of impurity peak and increasing of photoabsorption coefficient. The impurity peaks in $Ga_{1-x}Mn_xAs$ decrease under pressure increasing because the carriers were excited to conduction band by the effect of bond lengths reducing. The tendency of absorption coefficient of $Ga_{1-x}Mn_xAs$ in range of light-wavelength depends on size of impurity peak.

1. Introduction

The III–V binary compounds are widely used in the manufacture of semiconductor devices, especially Gallium Arsenide (GaAs) which used in the light-emitting diodes, field-effect transistors and photovoltaic cells [1]. GaAs is often performed as a substrate material for studying the effects of doping atoms that were grown on the thin film growth [2,3]. In previous studies of the high-pressure structures of GaAs, it is well known that the stable phase of GaAs at ambient pressure (0 GPa) is zinc blende (ZB) space group [4]. When pressure increasing, the GaAs–ZB structure transforms to an orthorhombic structure in space group *Cmcm* at 12–17 GPa [5–8]. The electronic properties of GaAs changed from semiconductor to semimetal [7] in the 1st phase transition (ZB→*Cmcm*), which is unsuitable condition for the application devices. At ambient pressure, the theoretical and experimental investigations have been performed for clarifying the structural, electronic, and magnetic properties of Mn-doped III–V semiconductors. The Mn effects on GaAs called diluted magnetic semiconductor are of great interest in previous studies. By using the molecular beam epitaxy (MBE) [9,10], it was found that the Mn impurities increase the Curie temperature, lattice constant and impurity band. The Mn impurities exhibit the carrier-induced ferromagnetism that can be controlled by changing the carrier density. Mn atoms preferably substitute on cation sites of GaAs which called (Ga,Mn)As [11,12]. Dietl et al. [13,14] have reported that the hole states of (Ga,Mn)As are extended in valence band, and mainly located within the inter-impurities region. By studying angle resolved photoemission spectroscopy, Okabayashi et al. [15] reported the presence of impurity band states above the extended valence band edge in $Ga_{0.965}Mn_{0.035}As$. The anticipated magnetic and electrical properties of $Ga_{1-x}Mn_xAs$ depended on trends in the binding energy of the Mn acceptor level and the strength of the p–d exchange [16]. Mn-derived impurity band that found in ab initio and dynamical mean-field theory approaches contained a strong exchange coupling spin states of Mn and GaAs [17–19]. Alberi et al. [20] suggested that the Mn-derived impurity band arises as the anticrossing interaction between the extended states of GaAs valence band and the strongly localized Mn states. For concentrations 3–12% of Mn, it was shown that the hole states are extended beyond the second As neighbours of the impurity [21,22]. By using tight-binding models, Turek et al. [23] found that Mn increases the number of holes for low concentrations ($x < 0.02$). For the higher concentrations of x, it exhibit qualitative changes including strong localization of eigenstates with energies close to the band edge. Milowska et al. [24] used the pSIC and the MLWF approaches for analyzing the Fermi level, gap regions of the (Ga,Mn)As density of states, hole localization and its chemical character. They presented that the hole states of 1% and 3% Mn replaced on Ga site have sp^3 character. Moreover, for dopings below 1%, the spin-unpolarized s-type impurity states segregate from the conduction band to the energy gap.

* Corresponding author.
E-mail address: prayoonsak@gmail.com (P. Pluengphon).

http://dx.doi.org/10.1016/j.ssc.2014.10.016
0038-1098/

In the literature review, we can see that Mn effects on GaAs–ZB at ambient pressure are widely studied much more. However, the high-pressure effects on (Ga,Mn)As are still incomplete. In this work, we focus to study on the electronic density of state (EDOS) and photoabsorption of GaAs under pressure at 0, 5 and 10 GPa. The magnitudes of EDOS peaks under pressure depend on the changing of lattice parameters and chemical bonds in (Ga,Mn)As. Mn substitution on Ga site generates electronic states in d orbitals. The impurity peaks occurred due to the available states of d orbitals from the impurity of Mn. Absorption coefficient depends on impurity peaks of EDOS.

2. Calculation details

In this work, ab initio calculations were performed by using density functional theory (DFT) implemented with CASTEP code [25,26]. The ground states properties such as density of electrons, effective potentials and total energies were evaluated by solving Kohn–Sham equations with the self-consistent field method. The ultrasoft pseudo-potentials were used for the scheme of pseudo-potentials. The pseudo-atomic calculations were performed at Ga $3d^{10}4s^24p^1$ and As $4s^24p^3$. For generating the $Ga_{1-x}Mn_xAs$ structures, the Mn atom was substituted on a Ga site in GaAs super cells. $Ga_{1-x}Mn_xAs$ structures were varied at $x=0.037$, 0.083 and 0.125 which obtained from substitution of Mn atom on a Ga site in the GaAs super cells sizes $2\times2\times2$, $2\times2\times3$ and $3\times3\times3$, respectively. For example, super cell size $2\times2\times2$ of GaAs in ZB was substituted by a Mn atom at a Ga site which called $Ga_{0.963}Mn_{0.037}As$ as shown in Fig. 1. It obtained from 8 cells of the GaAs primitive cell in ZB. Mn atom replaced on a Ga site at center of supercell.

The optimum cutoff energies for getting the total energy convergences of $Ga_{1-x}Mn_xAs$ in super cells $2\times2\times2$, $2\times2\times3$ and $3\times3\times3$ were found at 350 eV for the calculations of geometry optimizations, single point energies, electronic and optical properties. Forces on the optimized atomic positions were calculated by using the Hellmann–Feynman theorem [27]. We have observed phase transition from ZB to *Cmcm* [8] and found that phase transition from semiconductor (ZB) to nonsemiconductor (*Cmcm*) phase from our calculation occurred at 12 GPa, therefore; we selected to calculate the properties of (Ga,Mn)As at the pressure 0, 5 and 10 GPa. After we optimized the doped super cells, the EDOS and absorption coefficient of $Ga_{1-x}Mn_xAs$ were calculated by using the generalized-gradient approximation functional of Perdew–Burke–Ernzerhof (GGA–PBE) [28,29]. The condition in each direction of *k*-point sampling of Monkhorst–Pack grid size [30] is $1/k\leq0.05$ for calculations the properties of super cells. After we obtained the stable structures from the geometry optimizations, photoabsorption coefficient can be calculated from the imaginary part of complex refractive index which relate with the complex dielectric function ($\varepsilon=\varepsilon_1+i\varepsilon_2$). The real ($\varepsilon_1$) and imaginary parts ($\varepsilon_2$) of dielectric function evaluated from the matrix elements of the position operator that are required to describe the electronic transitions [31]. Photoabsorption coefficient is calculated by using Eq. (1) [32,33]

$$I(\omega)=2\omega\left(\frac{\sqrt{\varepsilon_1^2(\omega)+\varepsilon_2^2(\omega)}-\varepsilon_1(\omega)}{2}\right)^{1/2} \quad (1)$$

Photoabsorption coefficient indicates the fraction of energy lost by the wave when it passes through the material. For optical band gap discussion, it is well known that GGA–PBE functional gave the wrong band gap in semiconductor. The photoabsorption coefficient calculated from the GGA–PBE functional was compared with the screened exchange local-density approximation (sX-LDA) functional [34,35].

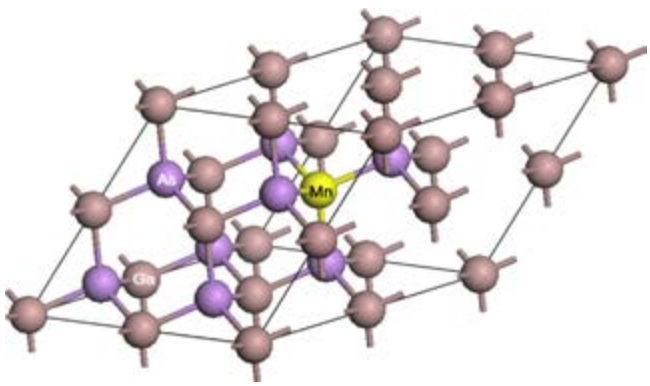

Fig. 1. Super cell size $2\times2\times2$ of GaAs in ZB was substituted by a Mn atom at a Ga site.

3. Results and discussion

In our calculation, we first compared the EDOSs of $Ga_{1-x}Mn_xAs$ ($x=0$, 0.037, 0.083 and 0.125) at ambient pressure (0 GPa) as shown in Fig. 2(a). Fermi levels of all $Ga_{1-x}Mn_xAs$ compounds were set at 0 eV, and the EDOSs in the varied sizes of super cells were divided per a formula unit of GaAs for comparing the electronic states. It was found that the Mn impurity reduces band gap of GaAs, and generates the peaks of EDOSs at near valence band maximum (VBM) and conduction band minimum (CBM), which is not found in undoped GaAs. The peaks at VBM and CBM in (Ga,Mn)As are the impurity bands in agreement with the previous studies [13–24]. In Fig. 2(a) and (b), the edge of VBM in all conditions was set at 0 eV so that size of impurity peak and band gap can be compared under pressure increasing. However, we found that the band gap of GaAs reduces due to Mn doping because the impurity peak in VBM (hole states) and in CBM (electron states) are extended into the band gap as shown in Fig. 2(c). This result supported that the impurity states segregate from the conduction band to the energy gap [24] and the hole states extend into gap [13,14,21,22,24]. Magnitudes of impurity peaks at VBM and CBM increase in strength with the Mn concentrations, which supported the result of the multiband tight-binding method [23]. These results confirm that the GGA–PBE calculation is in good agreement with previous studies at ambient pressure. When pressure increases in range of ZB phase up to 10 GPa, the variations of EDOSs are shown in Fig. 2(b). The impurity peaks of 3.70% (Ga,Mn)As are reduced under high pressure. However, the impurity peaks at a pressure 10 GPa still increase when the concentration of Mn increases. For high-pressure effects discussion, we analyze that the increasing of pressure reduces the magnitude of EDOS peaks due to the reducing of lattice parameters and chemical bonds in (Ga,Mn)As. Lattice parameters and chemical bonds of (Ga,Mn)As are reduced under high pressure as shown in Table 1 because the thermodynamics system got the external forces. When lattice parameters or sizes of primitive cells were reduced by pressure increasing, the densities of electronic states are spread out along axis of energy which same as the pressure effect of Na into Cu(In,Ga)Se_2 [36]. The flat of EDOSs due to the reducing of chemical bonds indicate the increasing of occupied states in conduction band but it reduces the EDOS at VBM. In Fig. 2(c), the example EDOSs of GaAs and (Ga,Mn)As are compared for explaining the occurred impurity peaks. By studying the 12.50% of Mn on Ga site with GGA–PBE functional, we found that the Mn impurity creates the electronic states in d orbitals near Fermi level. States of s orbitals increase at VBM. States of s and p orbitals extend in VBM when compared with the undoped condition. Band gap reduce in (Ga,Mn)As due to the

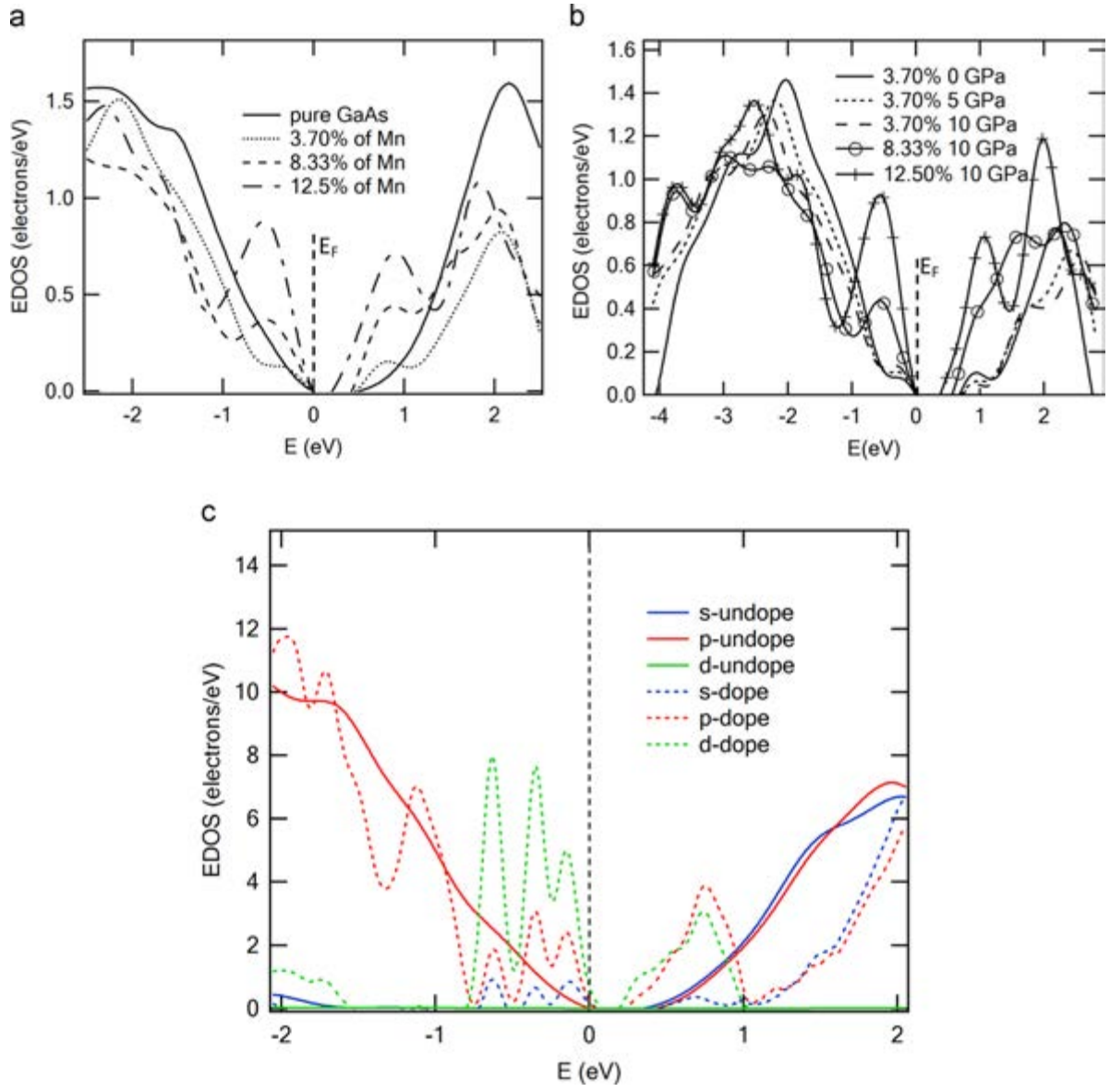

Fig. 2. (a) Comparisons the impurity peaks in EDOSs of (Ga,Mn)As at 0 GPa, which the Mn concentrations are 3.70%, 8.33% and 12.5%. (b) The impurity peaks of (Ga,Mn)As reduce under high pressure but it still increases in strength with the concentration at 10 GPa. (c) The partial density of states in s, p and d orbitals of GaAs and (Ga,Mn)As.

Table 1
The absorption coefficients at wavelength 450 nm and 650 nm (shown in the parenthesis) of (Ga,Mn)As under pressure at 0, 5 and 10 GPa and average bond lengths of Ga–As and Mn–As under pressure.

P (GPa)	Absorption coefficient ($\times 10^5$ cm^{-1}) at wavelength 450 and 650 nm				Average of Ga–As bond lengths (Å)	Average of Mn–As bond lengths (Å)		
	GaAs	3.70%Mn	8.33%Mn	12.50%Mn		3.70% Mn	8.33% Mn	12.50% Mn
0	7.43(3.94)	9.53(4.85)	10.30(6.16)	10.00(7.07)	2.490	2.357	2.349	2.339
5	6.46(2.76)	8.31(3.81)	9.47(5.19)	10.00(7.08)	2.421	2.307	2.301	2.298
10	5.67(1.90)	7.39(3.07)	8.71(4.46)	9.54(5.52)	2.383	2.260	2.259	2.258

peaks of d orbitals and p orbitals in CBM. We also compared the Mulliken atomic populations of (Ga,Mn)As and GaAs. Atomic population of Mn in (Ga,Mn)As is $s=0.52$, $p=0.54$ and $d=6.02$, while atomic population of Ga in doped GaAs translates from p to s orbitals when compared with undoped GaAs. The impurity peaks in (Ga,Mn)As from GGA–PBE functional occurred due to the transition states from p to s in Ga, the extended states in the band gap from VBM and CBM, and the generated d states from Mn atom. States of p orbitals in VBM both GaAs and (Ga,Mn)As dominate from As atoms which related with previous works [21,22]. While low concentration of Mn (1%) studied with the pSIC and the MLWF approaches [24], it was suggested that the hole density function resides mainly at the Mn–As complex, and it has mainly sp^3-character centred on the As-neighbors of Mn. When pressure increases up to the transition pressure of zinc blende to orthorhombic structures, we found that the energy gap of (Ga,Mn)As and GaAs are vanished and the properties of (Ga,Mn)As changed to nonsemiconductor.

For optical properties, it is well known that the optical band gap calculated from GGA–PBE functional gives the underestimated

solution because it used only local effective potential in term of correlation functional. Therefore, the photoabsorption implemented with sX-LDA functional that included the non-local potential was compared with the GGA–PBE result as shown in Fig. 3. Although, the sX-LDA functional improved the lowest photon energy for photoabsorption see in Fig. 3. But we found that the GGA–PBE and sX-LDA functionals gave the equivalent tendency of photoabsorption when compared with the experiment [37], but sX-LDA gave the better band gap or the lowest photon energy near the experiment [37]. However, the sX-LDA functional was performed by using norm-conserving potential. It requires the very large time for simulation especially in doping system when compare with GGA–PBE. GGA–PBE gives a good tendency and economizes the calculation time for photoabsorption calculation. From this research, we can conclude that the impurity of Mn gives the positive properties of GaAs such as increasing electronic states and photoabsorption coefficients. On the other hand, high pressure effect gives the negative properties for application devices from GaAs. For the absorption coefficients of $Ga_{1-x}Mn_xAs$ under pressure, it was found that the Mn impurity increases the photoabsorption of GaAs at a given pressure as shown in Fig. 4, especially as the region of visible light wavelength (400–700 nm). When we compare absorption coefficients between 0 and 10 GPa of 8.33% and 12.5% Mn, we can see that absorption coefficients reduce when pressure increasing. The absorption coefficients at wavelength 450 and 650 nm were compared as shown in Table 1. For the results of photoabsorption, we discuss that tendency of absorption coefficient relate with size of impurity peaks in EDOS. When the carrier concentrations (electrons and holes) at CBM and VBM are increased due to size of the Mn impurity, absorption coefficient which depends on probability of transition states of nearly free electrons from valence band to conduction band increases with sizes of impurity peaks. Under high pressure, the impurity peaks reduced due to the reducing of bond lengths in primitive cell; as a result, probability of transition states and photoabsorption are reduced by high-pressure effect. The average bond lengths of Ga–As and Mn–As presented in Table 1. When pressure increasing the bond lengths of Ga–As in a system are reduced due to pressure in all dimension. We found that when we substituted Mn on Ga site, the average of bond lengths of Mn–As is smaller than Ga–As. When Mn concentration increasing (at a constant of pressure), we found that bond lengths of Mn–As are reduced while size of impurity peak and photoabsorption coefficient are increased. We concluded that the impurity peak and photoabsorption coefficient depend on the relative bond length between Mn–As (impurity) and Ga–As (host).

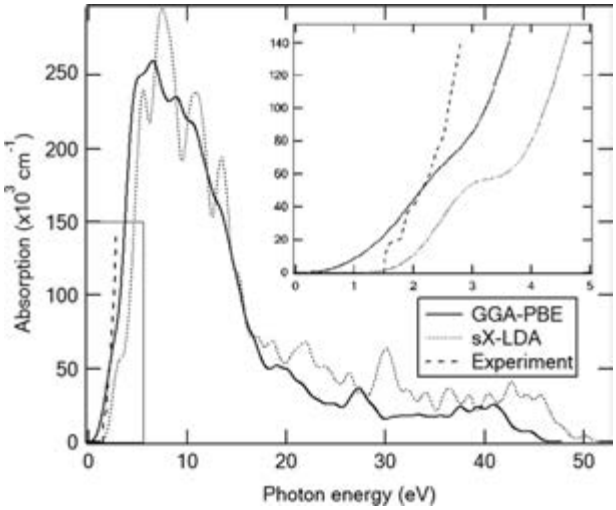

Fig. 3. Comparisons the absorption coefficients of GaAs at 0 GPa from the GGA–PBE, sX-LDA calculations and the experiment result [37] with photon energy 0.6–2.75 eV at 21 K.

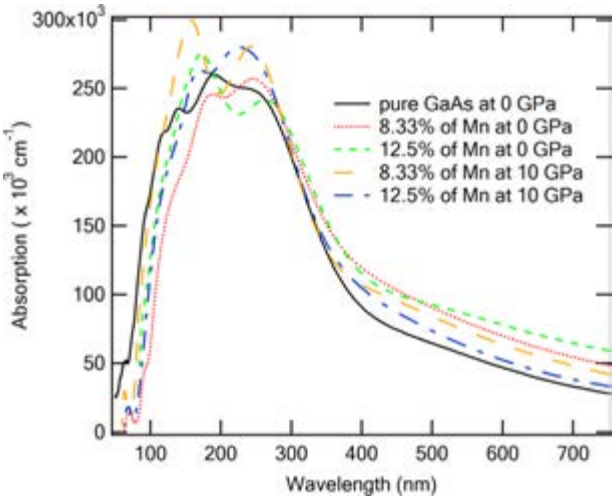

Fig. 4. Comparisons of photoabsorption coefficients in (Ga,Mn)As at 0 and 10 GPa.

4. Conclusions

In ZB phase of GaAs, the effects of Mn atom on Ga site of GaAs at the concentrations 3.70, 8.33 and 12.50% were investigated by using GGA–PBE functional. It was found that the Mn impurity reduces band gap of GaAs. The substitution of Mn on Ga site generates the impurity peaks at VBM and CBM. Mn substitution on Ga site generates electronic states in d orbitals. The impurity peaks in (Ga,Mn)As from GGA–PBE functional occurred due to the transition states from p to s in Ga and the generated d states from Mn atom. When lattice parameters and bond lengths in (Ga,Mn)As were reduced under pressure increasing, the electronic states of electrons are spread out in the axis of energy. As a result, the impurity peaks were reduced by high pressure effect. However, sizes of impurity peaks still increase in strength with Mn concentration at a given high pressure. For absorption coefficient in wavelength of visible light, the tendency of photo absorption depends on magnitude of impurity peaks.

Acknowledgments

P. Pluengphon would like to thank the financial support from Faculty of Science and Technology, Huachiew Chalermprakiet University. T. Bovornratanaraks acknowledges financial support from Asahi Glass Foundation, National Research Council of Thailand and Thailand Research Fund contract number DBG5280002. Computing facilities are supported by The National Research University Project of CHE and the Ratchadaphiseksomphot Endowment Fund (FW657B).

References

[1] F.L. Wu, S.L. Ou, R.H. Horng, Y.C. Kao, Sol. Energy Mater. Sol. Cells 122 (2014) 233.
[2] S. Kundu, T. Shripathi, P. Banerji, Solid State Commun. 151 (2011) 1881.
[3] M.M. Habchi, N. Tounsi, M. Bedoui, I. Zaied, A. Rebey, B. El Jani, Physica E 56 (2014) 74.
[4] A. Mujica, A. Rubio, A. Munoz, R.J. Needs, Rev. Mod. Phys. 75 (2003) 863.
[5] S.C. Yu, I.L. Spain, E.F. Skelton, Solid State Commun. 25 (1978) 49.
[6] S.T. Weir, Y.K. Vohra, C.A. Vanderborg, A.L. Ruoff, Phys. Rev. B: Condens. Matter 39 (1989) 1280.
[7] M. Durandurdu, D.A. Drabold, Phys. Rev. B: Condens. Matter 66 (2002) 045209.
[8] P. Pluengphon, T. Bovornratanaraks, S. Vannarat, U. Pinsook, Solid State Commun. 195 (2014) 26.
[9] L.X. Zhao, C.R. Staddon, K.Y. Wang, K.W. Edmonds, R.P. Campion, B.L. Gallagher, C.T. Foxon, Appl. Phys. Lett. 86 (2005) 071902.
[10] Y. Fukuma, H. Asada, M. Arifuku, T. Koyanagy, Appl. Phys. Lett. 80 (2002) 1013.

[11] S.J. Potashnik, K.C. Ku, S.H. Chun, J.J. Berry, N. Samarth, P. Schiffer, Appl. Phys. Lett. 79 (2001) 1495.
[12] K.M. Yu, W. Walukiewicz, T. Wojtowicz, I. Kuryliszyn, X. Liu, Y. Sasaki, J.K. Furdyna, Phys. Rev. B: Condens. Matter 65 (2002) 201303R.
[13] T. Dietl, et al., Science 287 (2000) 1019.
[14] T. Dietl, et al., Phys. Rev. B: Condens. Matter 63 (2001) 195205.
[15] J. Okabayashi, A. Kimura, O. Rader, T. Mizokawa, A. Fujimori, T. Hayashi, M. Tanaka, Phys. Rev. B: Condens. Matter 64 (2001) 125304.
[16] A.H. MacDonald, P. Schiffer, N. Samarth, Nat. Mater. 4 (2005) 195.
[17] Y. Zhang, S. Das Sarma, Phys. Rev. B: Condens. Matter 72 (2005) 125303.
[18] E.H. Hwang, S. Das Sarma, Phys. Rev. B: Condens. Matter 72 (2005) 035210.
[19] S. Sanvito, P. Ordejon, N.A. Hill, Phys. Rev. B: Condens. Matter 63 (2001) 165206.
[20] K. Alberi, K.M. Yu, P.R. Stone, O.D. Dubon, W. Walukiewicz, T. Wojtowicz, X. Liu, J.K. Furdyna, Phys. Rev. B: Condens. Matter 78 (2008) 159904.
[21] J. Park, et al., Physica B 281 (2000) 703.
[22] L.M. Sandratskii, et al., Phys. Rev. B: Condens. Matter 69 (2004) 195203.
[23] M. Turek, J. Siewert, J. Fabian, Phys. Rev. B: Condens. Matter 78 (2008) 085211.
[24] K. Milowska, et al., Chem. Phys. 430 (2014) 7.
[25] M.C. Payne, M.P. Teter, D.C. Allan, T.A. Arias, D. Joannopoulos, Rev. Mod. Phys. 64 (1992) 1045.
[26] M.D. Segall, P.L.D. Lindan, M.J. Probert, C.J. Pickard, P.J. Hasnip, S.J. Clark, M.C. Payne, J. Phys. Condens. Matter 14 (2002) 2717.
[27] R.P. Feynman, Phys. Rev 56 (4) (1939) 340.
[28] J.P. Perdew, J.A. Chevary, S.H. Vosko, K.A. Jackson, M.R. Pederson, D.J. Singh, C. Fiolhais, Phys. Rev. B: Condens. Matter 46 (1992) 6671.
[29] J.P. Perdew, K. Burke, M. Ernzerhof, Phys. Rev. Lett. 77 (1996) 3865.
[30] H.J. Monkhorst, J.D. Pack, Phys. Rev. B: Condens. Matter 13 (1976) 5188.
[31] A.J. Read, R.J. Needs, Phys. Rev. B: Condens. Matter 44 (1991) 13071.
[32] J. Choy, J. Phys. Chem. Solids 52 (2001) 545.
[33] Z.B. Li, X. Wang, K.L. Yao, Solid State Commun. 150 (2010) 1514.
[34] A. Seidl, A. Görling, P. Vogl, J.A. Majewski, M. Levy, Phys. Rev. B: Condens. Matter 53 (1996) 3764.
[35] S. Chawla, A.G. Voth, J. Chem. Phys. 108 (1998) 4697.
[36] P. Pluengphon, T. Bovornratanaraks, S. Vannarat, U. Pinsook, J. Phys. Condens. Matter 24 (2012) 095802.
[37] M.D. Sturgk, Phys. Rev 127 (1962) 768.